Article

Outcome One Year After Acetabular Rim Extension Using a Customized Titanium Implant for Treating Hip Dysplasia in Dogs

Irin Kwananocha , Joëll Magré , Amir Kamali , Femke Verseijden , Koen Willemsen , Yuntao Ji , Bart C.H. van der Wal , Ralph J.B. Sakkers , Marianna A. Tryfonidou , Björn P. Meij *

Posted Date: 4 July 2024

doi: 10.20944/preprints202407.0468.v1

Keywords: hip dysplasia; dog; customized implant; 3D printed implant; femoral head coverage; acetabular rim extension; ACE-X

Article

Outcome One Year After Acetabular Rim Extension Using a Customized Titanium Implant for Treating Hip Dysplasia in Dogs

Irin Kwananocha [1,2], Joëll Magré [3,4], Amir Kamali [1], Femke Verseijden [1], Koen Willemsen [3,4], Yuntao Ji [5], Bart C.H. van der Wal [3], Ralph J.B. Sakkers [3], Marianna A. Tryfonidou [1] and Björn P. Meij [1,*]

1 Department of Clinical Sciences, Faculty of Veterinary Medicine, Utrecht University, Yalelaan 1, Utrecht, 3584 CL, The Netherlands; i.kwananocha@uu.nl; s.a.kamali@uu.nl; f.verseijden@uu.nl; m.a.Tryfonidou@uu.nl

2 Research and Academic Service, Faculty of Veterinary Medicine, Kasetsart University, 50 Ngamwongwan Rd., Lat Yao, Chatuchak, Bangkok, 10900, Thailand; i.kwananocha@uu.nl

3 Department of Orthopedics, University Medical Center Utrecht, Heidelberglaan 100, Utrecht, 3584 CX, The Netherlands; J.Magre-2@umcutrecht.nl; k.willemsen-3@umcutrecht.nl; B.C.H.vanderwal@umcutrecht.nl; .sakkers@umcutrecht.nl

4 3D Lab UMC Utrecht, Division of Surgical Specialties, University Medical Center Utrecht, Heidelberglaan 100, Utrecht, 3584 CX, The Netherlands; j.magre-2@umcutrecht.nl; k.willemsen-3@umcutrecht.nl

5 Department of Earth Sciences, Faculty of Geosciences, Utrecht University, Princetonlaan 8a, Utrecht, 3584 CB, the Netherlands; y.ji@uu.nl

* Correspondence: b.p.meij@uu.nl

Simple Summary: Hip dysplasia is prevalent among young dogs, affecting approximately 16% of the overall dog population, causing pain, exercise intolerance, and potentially leading to severe osteoarthritis. Current surgical interventions, such as pelvic osteotomies and total hip replacement, have limitations and high complications. To address this, a personalized 3D-printed titanium implant was developed for dorsal ACEtabular rim eXtension (ACE-X), enhancing hip joint coverage and reducing hip laxity. In a previous short-term study spanning 3 months, the ACE-X implant demonstrated promising results: improved femoral head coverage, decreased pain-related activities based on owner questionnaires, and facilitated rapid recovery. This study aimed to offer a thorough analysis of clinical outcomes following a 1-year follow-up period. The analysis encompassed radiographic measurements, force plate analysis, owner questionnaires, an assessment of bone-implant osseointegration, as well as the identification and documentation of any complications encountered during the study period. By evaluating the long-term efficacy and safety of the ACE-X implant, this research contributes valuable insights into the management of hip dysplasia in dogs, potentially offering a novel and effective treatment option for this prevalent orthopedic condition.

Abstract: The ACEtabular rim eXtension (ACE-X) implant is a custom-made 3-dimensional-printed titanium device designed for the treatment of canine hip dysplasia. Thirty-four dogs (61 hips) underwent ACE-X implantation, and assessments were conducted using computed tomography, force plate analysis, Ortolani's test, and Helsinki Chronic Pain Index (HCPI) questionnaires at five intervals: pre-operative day, surgery day, 1.5-month, 3-month, and 12-month follow-up. Statistically significant increases in femoral head coverage with negative Ortolani subluxation test were observed immediately after surgery and persisted throughout the study. Osteoarthritis (OA) scores remained stable, but osteophyte size significantly increased between the surgery day and the 12-month follow-up, especially in hips with a baseline OA score of 2 compared to those with a score ofForce plate data showed no significant changes during the study. The HCPI demonstrated a significant decrease in pain score from pre-operative value to 6-week follow-up and gradually decreased over time. Major complications were identified in 6 hips (9.8%) of 4 dogs. In conclusion, the ACE-X implant effectively increased femoral head coverage, eliminated subluxation, and provided long-term pain relief with minimal complications, benefiting over 90% of the study population. The study supports the ACE-X implant as a secure and valuable treatment for canine hip dysplasia.

 doi:10.20944/preprints202407.0468.v1

Keywords: hip dysplasia; dog; customized implant; 3D printed implant; femoral head coverage; acetabular rim extension; ACE-X

1. Introduction

Canine Hip Dysplasia (CHD) is a prevalent developmental orthopedic condition that affects young dogs, especially those of medium to large breeds, with an overall prevalence of 16% [1]. CHD leads to instability (laxity) of the hip joint and hip pain. Owners may observe abnormal gait and lameness after exercise, typically becoming noticeable between 4 and 10 months of age [2]. This condition occurs due to continuous abnormal movement of the femoral head (ball), which causes deformation of the acetabulum (socket). The long-term consequence of this joint laxity is the gradual loss of cartilage and the early onset of osteoarthritic changes in the joint. Conservative management alone cannot halt the progression of clinical dysplastic disease; therefore, early surgical intervention is necessary to restore the joint's normal weight-bearing forces and prevent or slow down osteoarthritic changes.

Current surgical options for early-stage CHD include juvenile pubic symphysiodesis (JPS), double or triple pelvic osteotomy (DPO/TPO), intertrochanteric osteotomy, and dorsal acetabular rim arthroplasty (DARthroplasty). These techniques aim to reduce hip joint laxity by increasing the weight-bearing surface, thereby preventing further joint damage [3–7]. However, each of these techniques has its inherent disadvantages such as upper age limits for surgery (JPS and DPO), invasiveness (DPO/TPO), risk of complications (TPO), and suboptimal outcomes in all procedures [3,8–11].

To offer an alternative treatment option with a more predictable outcome, faster recovery time, and lower risk of harm, a novel personalized surgical technique for early-stage CHD was developed. This new technique utilizes a patient-specific 3-dimensional (3D) printed shelf implant for dorsal Acetabular Rim Extension (ACE-X). The ACE-X implant is designed based on computed tomography (CT) imaging of the pelvis and hip joints of individual dogs to extend the dorsal acetabular rim optimally and provide sufficient coverage of the femoral head. In previous proof-of-concept pilot studies [12] involving asymptomatic dogs with radiographic hip dysplasia (n = 3) and in a short-term (3 months) clinical trial [13] in these 34 dogs with hip dysplasia (HD), the ACE-X implant reduced hip laxity and restored coverage of dysplastic hip joints. This new technique, without the use of osteotomies, was associated with low postoperative morbidity and fast gait recovery, allowing bilateral procedures in one operative session. The present study was designed to investigate the outcomes of the ACE-X implant on hip laxity and osteoarthritic changes in client-owned dogs with HD over an extended duration. Clinical examinations, gait analysis using force plates, owners' questionnaires, and CT scans were used to evaluate the efficacy of the ACE-X implant up to 12 months postoperatively. Furthermore, successful osseointegration of the ACE-X implant, crucial for implant stability, and long-term implant survival, was investigated.

2. Materials and Methods

2.1. Study Design and Overview

This study is a prospective non-randomized unblinded self-controlled clinical trial involving client-owned dogs that underwent surgery for ACE-X implantation at the Department of Clinical Sciences, Faculty of Veterinary Medicine, Utrecht University between 2019 andApproval for the study was obtained from the Veterinary Clinical Studies Committee, Utrecht University, Utrecht, The Netherlands. Throughout the study, the dogs remained under the supervision and care of their owners, who were informed about the study's objectives, the surgical ACE-X procedure, available alternative treatments, the treatment plan, and all potential complications associated with ACE-X treatment (e.g., infection, implant failure, neurological deficits, and others). All owners provided informed written consent before their dogs participated in the study.

 doi:10.20944/preprints202407.0468.v1

A total of 34 dogs (61 studied hips) were monitored during a 12-month follow-up period. During this period, the dogs were examined at five designated time points: the pre-operative day (visit 1), the day of surgery (visit 2), 1.5 months follow-up (visit 3), 3 months follow-up (visit 4), and 12 months follow-up (visit 5). Different clinical observations, including imaging, force plate gait analysis, Ortolani's test, and the Helsinki Chronic Pain Index (HCPI) questionnaires, were performed at each visit (Table 1).

Table1. Study outline.

Evaluation	Preoperative day (Visit 1)	Day of surgery (Visit 2)	1.5 months follow-up (Visit 3)	3 months follow-up (Visit 4)	12 months follow-up (Visit 5)
Radiograph	x[a]	x	x	-	-
CT scan	x[b]	x[b]	-	x[b]	x[b]
Osteophyte size*	x	x	-	x	x
OA scoring**	x[a,b]	x	-	x	x
FCI scoring	x	-	-	-	-
Force plate gait analysis	x	-	x	x	x
HCPI	x	-	x	x	x
Ortolani's test	x	x	x	x	x

CT; computed tomography, OA; osteoarthritis, FCI; Fédération Cynologique Internationale, HCPI; Helsinki chronic pain index., * Osteophyte size was measured on CT scans at 3 locations: femoral neck and the cranial and caudal acetabular rim. ** At intake, OA was scored using preoperative radiograph [a] for inclusion. For monitoring, OA score was based on the maximum osteophyte size determined through CT measurements [b].

Client-owned dogs older than 6 months, exhibiting a positive Ortolani's test under sedation and radiographic signs of hip dysplasia within the Fédération Cynologique Internationale (FCI) score range of B (borderline) to E (severe) [14–17], as well as radiographic osteoarthritis (OA) scores falling between 0 (osteophyte size 0 mm) and 1 (osteophyte size 0.1 – 2 mm) [18], were considered eligible for participation in the study. The FCI and intake OA scores were categorized based on preoperative radiographs obtained during the inclusion process, either conducted at the referring hospital or Utrecht University. Individuals were excluded from study participation if they exhibited an open acetabular growth plate, a negative Ortolani's test, moderate to severe osteoarthritis (indicated by an intake OA score ≥ 2 or osteophyte size > 2.0 mm), systemic disease, luxoid hip condition, neurological deficits, or a history of previous hip surgery. Preoperative CT planning was performed for the development of a personalized ACE-X implant. Mimics (version 24, Materialise, Leuven, Belgium) was used for segmentation of the DICOM files and 3-Matic (version 16, Materialise, Leuven, Belgium) for implant design at the 3D Lab of University Medical Centre Utrecht as described previously by Willemsen et al. and Kwananocha et al. [12,13,19]. The ACE-X implant was positioned extracapsular of the hip joint, over the upper edge of the dorsal acetabular rim, and secured using four screws on the iliac body (Figure 1). The duration between the day the preoperative CT was performed (visit 1) and the day of surgery (visit 2) was set as the lead time.

 doi:10.20944/preprints202407.0468.v1

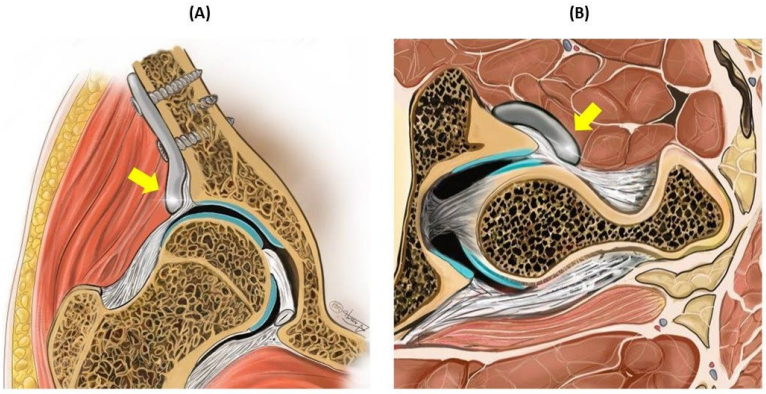

Figure 1. Schematic representation of the dysplastic hip joint with the ACEtabular rim eXtension (ACE-X) implant in the coronal plane **(A)** and transverse plane **(B)**. The ACE-X implant (indicated by the yellow arrow) was positioned extracapsular of the hip joint and extended the dorsal acetabular rim, thereby increasing femoral head coverage.

2.2. Radiographic and Clinical Assessment

2.2.1. Radiographic Measurements:

The Norberg Angle (NA), linear percentage of femoral head overlap (LFO), and percentage of femoral head coverage (PC) were evaluated from coronal CT scans following the methodology outlined in the earlier short-term report [13] during visits 1, 2, 4, andConcurrently, the progression of OA was assessed based on the maximal thickness of osteophytes detected at three distinct locations on CT: the cranial and caudal acetabular rim, and the femoral neck. These assessments were conducted using both coronal and transverse CT scans. The OA scoring system consisted of four distinct categories: OA score 0 (osteophyte size of 0 mm), 1 (osteophyte size 0.1 to 2 mm), 2 (osteophyte size 2.1 to 5 mm), and 3 (osteophyte size > 5 mm) [18]. The baseline value for the OA score and the measured osteophyte size were established from the immediate postoperative CT scan at visitThe radiographic measurements were performed using the Xero Viewer software (AGFA HealthCare, Mortsel, Belgium) by a single observer (IK).

2.2.2. Force Plate Gait Analysis:

Ground reaction forces (GRFs) were assessed using a single force plate (Kistler type 9261, Kistler Instrument AG, Winterthur, Switzerland) embedded at the midpoint of an 11-meter-long walkway during visits 1, 3, 4, andThe dogs were led on a leash across the force plate, maintaining a consistent velocity between 0.8 and 1.3 m/s. For each limb's side, the first 4 to 10 valid trials were recorded, and then averaged. A valid trial was defined as the forelimb being succeeded by the ipsilateral hind limb contacting the force plate during the dog's walking movement. GRFs, including breaking force, propulsion force, peak vertical force (PVF), vertical impulse (VI), and pelvic (P) and thoracic (T) indices (P/T index), were calculated and subsequently normalized relative to the dog's body weight.

2.2.3. The Helsinki Chronic Pain index (HCPI) Questionnaire:

During visits 1, 3, 4, and 5, owners were provided with the HCPI questionnaire [20]. This survey consisted of 11 inquiries, each utilizing a 5-point descriptive scale (scoring from 0 to 4). Subsequently, an overall score was calculated, ranging from 0 toScores falling between 0 and 1 within each question indicated typical dog behavior or movement while scores ranging from 2 to 4 suggested atypical behavior or movement. A total score of less than 6 denoted the absence of pain, while a cumulative score exceeding 11 signified the presence of chronic pain. Scores between 6 and 11 constituted an indeterminate zone, as established by previous studies [20,21]. In this study, each dog's overall index score was transformed into a percentage by dividing it by the maximum possible score based on the answered questions. This transformation allowed for further analysis, wherein a sum score over 25%

 doi:10.20944/preprints202407.0468.v1

indicated chronic pain, a total score under 13.6% indicated the absence of pain, and scores between 13.6% and 25% were categorized as inconclusive.

2.2.4. Ortolani's Test:

The Ortolani's test was performed while the dog was in lateral recumbency, under either sedation or general anesthesia, during each of the five scheduled visits.

2.3. Histopathology and Bone Implant Contact

In cases where dogs experienced complications necessitating revision surgery, the ACE-X implants were removed and the soft tissues surrounding the hip joint were collected for histopathological examination as described below. When total hip replacement (THR) was performed, the femoral head was obtained for histopathological analysis after femoral head ostectomy. Soft tissue biopsies were fixed in 10% neutral buffered formalin (NBF, pH 7.26) for 48 hours, then processed and embedded in paraffin. Formalin-fixed femoral head specimens underwent decalcification in 10% Ethylenediaminetetraacetic acid (EDTA) for 3 months. The paraffin-embedded soft tissue and bone samples were sectioned into 5 µm thick slices and stained with hematoxylin and eosin (H&E). Histological sections were examined by an independent pathologist (AK), utilizing light microscopy (Olympus BX51; Olympus, Tokyo, Japan). To assess osseointegration, removed ACE-X implants were preserved in 10% neutral buffered formalin for a minimum of 6 months. Subsequently, these specimens underwent analysis using a three-dimensional (3D) X-ray microscope (Zeiss Xradia 610 Versa, Germany) as well as histopathological examination.

For imaging, the implants were affixed to a turntable capable of vertical rotation, enabling optimal sample positioning. CT imaging was conducted using a ZEISS Xradia 610 Versa 3D X-ray Microscope (Carl Zeiss X-ray Microscopy Inc., Germany) situated in the Multi-scale Imaging and Tomography Facility (MINT) at Utrecht University. Multiple series of projections were acquired for each sample, with the number of projections per scan ranging from 1,201 to 2,401 to achieve a high signal-to-noise ratio within an acceptable scanning duration. Image reconstructions were performed using the 'Reconstructor Scout-and-Scan' software developed by Zeiss, with pixel sizes ranging from 2.4 µm to 7.74 µm. Incident X-rays generated using a voltage of 140 kV and 21 W power, without a source filter, optimized the transmittance of the projection images, maximizing the grey level contrast between the metal implant, bone tissue, and air, making them clearly distinguishable in the reconstructed images. Image thresholding and figure plotting were conducted using TXM3DViewer software (Carl Zeiss X-ray Microscopy Inc., Germany).

For histopathology, the formalin-fixed explanted implant and interconnected bone was dehydrated using a graded series of ethanol solutions. Subsequently, the sample was infiltrated with a plastic embedding substance (polymethyl methacrylate (PMMA) monomers and initiators) in a desiccator environment to achieve proper dehydration and optimum penetration. The embedding process involved carefully placing the dehydrated and PMMA-infiltrated specimen into the embedding mold, followed by polymerization through temperature and cure time control. A 5 mm section was removed from one side of the block using a diamond-coated saw to access the middle of the sample and verify the porous structure of the explanted implant. The specimen was then sliced to 80 µm thickness using a saw microtome (Leica SP 1600, Leica Microsystems, Wetzlar, Germany). The sections were stained with methylene blue and acid fuchsin for evaluation under light microscopy (Olympus BX53, Olympus, Tokyo, Japan).

2.4. Statistical Analysis

Normality was assessed using Q-Q plot (SPSS version 28, IBM, NY, USA). Radiographic measurements (i.e., NA, LFO, PC, and osteophyte size), HCPI, and GRFs were analyzed using generalized linear mixed models. Results of OA scores were evaluated using related-samples Friedman's two ways analysis of variance. The Kruskal-Wallis test was employed to assess changes in osteophyte size over time among dogs with different baseline OA scores and FCI scores. Bonferroni

 doi:10.20944/preprints202407.0468.v1

post-hoc tests were conducted to correct for differences between time periods and OA score groups. Values with $p < 0.05$ were considered statistically significant.

3. Results

The patient demographics were previously detailed in an earlier publication about the short-term results [13]. In summary, this study involved 34 client-owned dogs, encompassing a total of 61 dysplastic hips. The cohort comprised 24 males and 10 females, with a median age of 12 months (7 – 38 months) and a median body weight of 27.3 kg (12 – 86 kg). Among them, 7 dogs underwent unilateral hip surgery, while 27 dogs underwent surgery on bilateral hips. Among the dogs with bilateral hip surgery, seven underwent the procedure in two separate sessions, with a median interval of 92 days (range: 56 – 524 days) between the two sides.

The number of various examinations conducted at different time points, including the preoperative day (visit 1), day of surgery (visit 2), 1.5 months (visit 3), 3 months (visit 4), and 12 months (visit 5) of follow-up (Table 2, Figure 2). The median lead time between the preoperative day and the day of surgery was 74 days (46 – 158 days). The median durations between the day of surgery and 1.5 months, 3 months, and 12 months follow-up were 45 days (range: 24 – 92 days), 99 days (range: 68 – 289 days), and 386 days (range: 270 – 553 days), respectively. Over the 12-month study period, five hips (in three dogs) were excluded at 6 months (hip no. 34), 7 months (hip no. 37), 9 months (hip no. 23), 10 months (hip no. 25), and 12 months (hip no. 24) after surgery due to implant failure (hips no. 23, 34 and 37) and severe osteoarthritis progression (hip no. 24 and 25). The other hips showed positive outcomes in the 12-month duration with a representative example demonstrated in Figure 2.

Table 2. Clinical tests were conducted per visit. The numbers are displayed as performed tests/total tests (percentage).

Evaluation	Visit 1	Visit 2	Visit 3 (24 – 92 days)	Visit 4 (68 - 289 days)	Visit 5 (270 - 553 days)
CT scan*	61/61 (100%)	61/61 (100%)	-	50/61 (82%)	45/61 (74%)
OA scoring*	61/61 (100%)	61/61 (100%)	-	50/61 (82%)	45/61 (74%)
Force plate*	51/61 (84%)	-	54/61 (89%)	46/61 (75%)	44/61 (72%)
HCPI**	33/41 (80%)	-	21/41 (51%)	23/41 (56%)	25/37[ǂ] (68%)
Ortolani's test*	61/61 (100%)	61/61 (100%)	55/61 (90%)	50/61 (82%)	45/61 (74%)

HCPI: Helsinki chronic pain index. *The quantity represents the number of hips. **The quantity represents the number of dogs. [ǂ] The four dogs that underwent surgery on bilateral hips, with a 3-month interval in between, returned for a 1-year follow-up to assess both hips in a single visit, bringing the total number to 37 dogs.

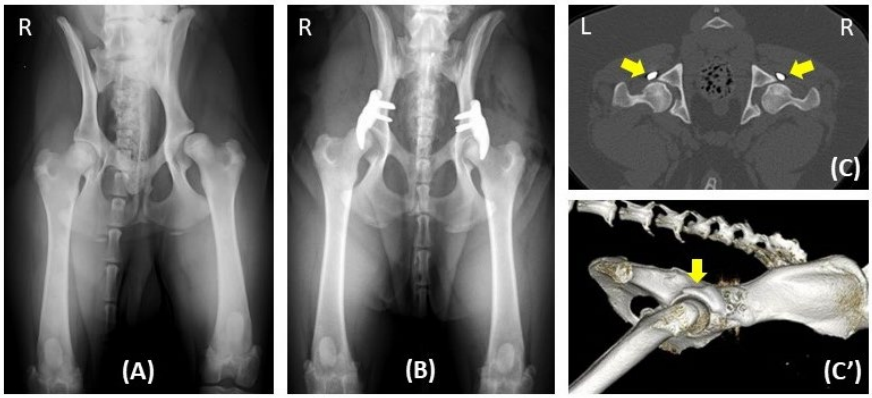

 doi:10.20944/preprints202407.0468.v1

Figure 2. One year radiographic follow-up in a dog with hip dysplasia undergoing bilateral ACEtabular rim eXtension (ACE-X) surgery. Preoperative radiography **(A)** reveals hip laxity without evidence of osteoarthritis (OA). Immediate postoperative radiography **(B)** after bilateral ACE-X implantation shows minimal development of OA (Morgan line) during the lead time. Transverse CT of the hips **(C)** and 3D reconstruction of the right lateral pelvis **(C')** at the 1-year follow-up highlight the rim extension part of the ACE-X implants (yellow arrow), extending the dorsal acetabular rim and enhancing femoral head coverage without progression of OA.

3.1. Assessment of Hip Joint Laxity Testing (Ortolani's test)

At intake, all 61 hips exhibited a positive Ortolani sign; however, 6 hips were found a negative Ortolani's test during preoperative evaluation on the day of surgery. After ACE-X implantation, two hips exhibited a positive Ortolani's test immediately postoperative (hip no. 36) and at 1.5-month follow-up (hip no. 56). By the 12-month follow-up, hip number 56 had transitioned to a negative Ortolani's test. However, another hip (hip no. 53) displayed a positive Ortolani's test at 12-month follow-up (visit 5). Thus, the presence of a positive Ortolani's test was noted in two out of the 55 hips during visit 5.

3.2. Radiographic Outcomes

The FCI score was determined by two national hip dysplasia screening panelists (MT and BM) using ventrodorsal hip extension radiographs taken preoperatively, revealing FCI scores of B (7 hips), C (8 hips), D (22 hips), and E (24 hips). The NA, LFO, and PC measures using coronal CT significantly increased at visits 2, 4, and 5 compared to visit 1 ($p < 0.001$) (Table 3).

The median OA scores and mean (± SD) osteophyte size at visit 1 (1; range 0 – 2 and 1.26 ± 0.84 mm, respectively) were significantly increased when compared to visit 2 (1; range 0 – 2 and 1.86 ± 1.28 mm, respectively) ($p < 0.001$ and $p < 0.05$) as previously reported in the short-term results [13]. This study assessed the OA scores based on immediate post-operative CT scans at visit 2, which served as the baseline value. The median OA score did not significantly change between visit 2 (1; range 0 – 2), visit 4 (2; range 0 – 3), and visit 5 (2; range 0 – 3) ($p = 0.115$) (Figure 3A). However, the mean (± SD) osteophyte size increased significantly between visit 2 (1.8 ± 1.3 mm) and visit 5 (2.7 ± 2.0 mm) ($p = 0.028$) (Figure 3B). The average (± SD) increases in osteophyte size over the 12-month period from visit 2 to visit 5 significantly varied between the group with a baseline OA score 2 (1.6 ± 1.3 mm) and the group with a baseline OA score 1 (0.2 ± 0.6 mm) ($p < 0.001$). However, there was no significant difference observed between the group with a baseline OA score 1 (0.2 ± 0.6 mm) and the group with a baseline OA score 0 (0.8 ± 1.2 mm) ($p = 0.181$) as illustrated in Figure 3C. Additionally, there was no significant difference observed in the mean increase in osteophyte size between hips with FCI scores B (0.8 ± 1.4 mm), C (0.5 ± 0.9 mm), D (0.6 ± 0.9 mm), and E (1.6 ± 1.4 mm) ($p = 0.097$) as depicted in Figure 3D.

Preprints.org (www.preprints.org) | NOT PEER-REVIEWED | Posted: 4 July 2024 doi:10.20944/preprints202407.0468.v1

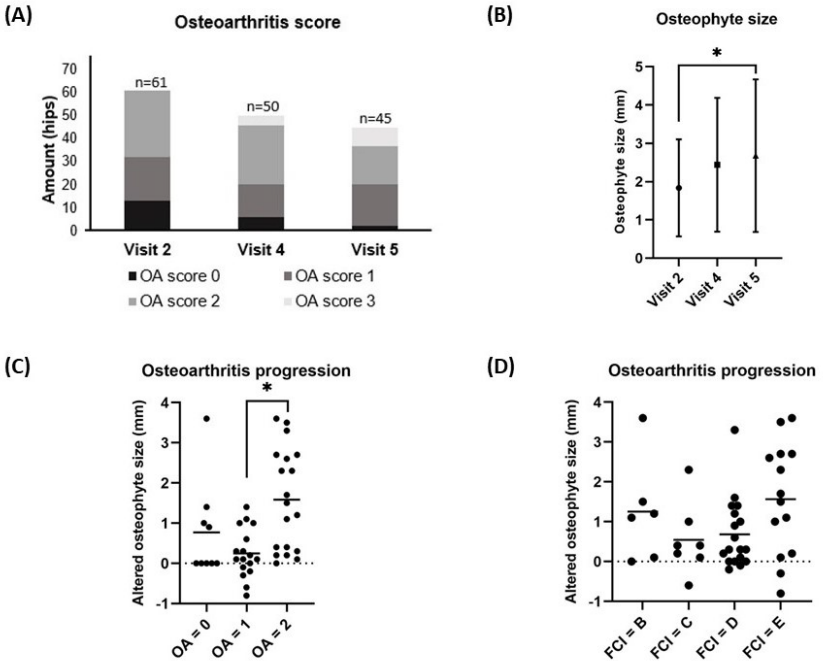

Figure 3. The changes in osteoarthritis (OA) score **(A)** and osteophyte size **(B)** from the baseline value (visit 2) to the 12-month follow-up (visit 5), and the comparison of osteophyte size growth between visit 2 and visit 5 grouped by baseline OA score **(C)** and FCI score **(D)** are depicted. **(A)** Each bar represents the number of hips in each OA score at each time point. **(B)** Each dot represents the mean osteophyte size ± SD at each time point. **(C, D)** Each dot represents an individual change in osteophyte size over 12 months, while each line illustrates the mean osteophyte size change over 12 months. *p-value of < 0.05 was considered significant using Bonferroni correction for multiple tests. OA score progression was based on CT measurements of osteophytes from baseline (visit 2) to visitFCI score was done on pre-operative radiographs at visit 1.

Table 3. Results from dogs with hip dysplasia that underwent acetabular rim extension were assessed preoperatively (visit 1), immediately postoperatively (visit 2), at 3 months (visit 4), and at 12 months (visit 5) follow-up.

Outcome measurements		Visit 1	Visit 2	Visit 3	Visit 4	Visit 5	p-value
CT-scan measurements (Mean ± SD)	NA (°)	88.5 ± 12.6 [a]	137.6 ± 19.2 [b]	-	134.3 ± 19.0 [b]	131.5 ± 17.8 [b]	< 0.000
	LFO (%)	24.3 ± 16.2 [a]	83.8 ± 16.4 [b]	-	79.8 ± 18.2 [b]	78.1 ± 17.4 [b]	< 0.001
	PC (%)	34.7 ± 17.3 [a]	82.3 ± 20.0 [b]	-	80.2 ± 18.8 [b]	77.4 ± 19.5 [b]	< 0.001
GRFs (Mean ± SD)	PVF (%BW)	40.9 ± 5.8	-	38.9 ± 4.8	39.8 ± 5.4	40.9 ± 6.0	0.166
	P/T index	0.62 ± 0.1	-	0.58 ± 0.1	0.59 ± 0.1	0.61 ± 0.1	0.067
	VI (%BW.s)	14.2 ± 3.0	-	13.8 ± 3.4	14.3 ± 3.0	14.6 ± 4.0	0.705
	Breaking force (%BW)	6.38 ± 1.7	-	6.11 ± 1.6	6.41 ± 1.5	6.43 ± 1.9	0.726
	Propulsion force (%BW)	6.64 ± 1.5 [a]	-	5.99 ± 1.6 [a,b]	5.78 ± 1.4 [b]	5.58 ± 1.9 [b]	0.007

 doi:10.20944/preprints202407.0468.v1

HCPI (%) (Mean ± SD)	30.29 ± 13.55 [a]	-	21.86 ± 12.39 [b]	19.37 ± 11.54 [b]	18.27 ± 12.0 [b]	0.002

NA: Norberg angle, LFO: linear percentage of femoral head overlap, PC: percentage of femoral head coverage, SD: standard deviation, GRFs: ground reaction forces, PVF: peak vertical force, P/T index: pelvic/thoracic index, VI: vertical impulse, BW: body weight, s: second, [a,b] p-value < 0.05 based on post-hoc Bonferroni correction, p-value < 0.05 from generalized linear mixed model. HCPI (%) = 100% x (total index score/maximum possible index score of the answered questions).

3.3. Kinetic Gait Analysis

The GRFs were measured preoperatively (n = 51), at 1.5 months (n = 54), 3 months (n = 46), and 12 months (n = 44) follow-up. A significant change was not observed between each visit for PVF (p = 0.166), P/T index (p = 0.067), VI (p = 0.705), and breaking force (p = 0.726). However, propulsion force differed significantly between the preoperative evaluation (visit 1) and the follow-up evaluations at 3 months (visit 4) and 12 months (visit 5) (p = 0.007) (Table 3).

3.4. Owner Assessment of Pain-Related Behavior

Owner assessments of pain-related behavior were collected through HCPI questionnaires at various time points for each individual dog, regardless of whether they had undergone unilateral or bilateral ACE-X implantation. The number of returned questionnaires is presented in TablePain-related behavior significantly reduced over time, when comparing the preoperative assessment (30%) with the assessments at 1.5 months (22%), 3 months (19%), and 12 months (18%) follow-up (p = 0.002) (Table 3).

3.5. Complications

In the previous short-term study, 3 hips (4.9%) had perioperative complications, including problems with imperfect implant positioning in 2 hips and screw misalignment in 1 hip [13], whereas 9 hips (14.8%) had postoperative issues in this long-term study. Regarding postoperative complications, 3 hips (hips no. 42, 46, and 47) from 2 dogs, accounting 4.9% of the cases, experienced minor issues, notably intermittent lameness attributed to OA progression. These cases responded well to pain medication and did not require revision surgery during the study period. Major complications were observed in 6 hips (9.8%) from 4 dogs (Table 4), including ACE-X implant failure (hip no. 34), screws breakage (hips no. 23 and 37), substantial osteoarthritis progression with severe lameness (hips no. 24 and 25), and osteomyelitis due to septic arthritis (hip no. 53). These major complications occurred at various intervals post-operation, ranging from 6 to 17 months following the initial surgery.

In one case, implant failure occurred bilaterally (hips no. 23 and 34) in a dog that underwent staged bilateral ACE-X implantation with a two-month interval between each hip procedure (Figure 4A). Unfortunately, the dog experienced bilateral humeral condyle fractures five months post-operation on the second hip (hip no. 34), requiring plate and screw fixation (Figure 4B). Subsequently, the ACE-X implant in the right hip (hip no. 34) and screws in the left hip (hip no. 23) broke and severe OA progression was evident in both hips (Figure 4C), necessitating revision surgery involving implant removal and total hip replacement (THR) at 9 months and 15 months post ACE-X implantation (Figure 4D), respectively (Table 4: Dog 1).

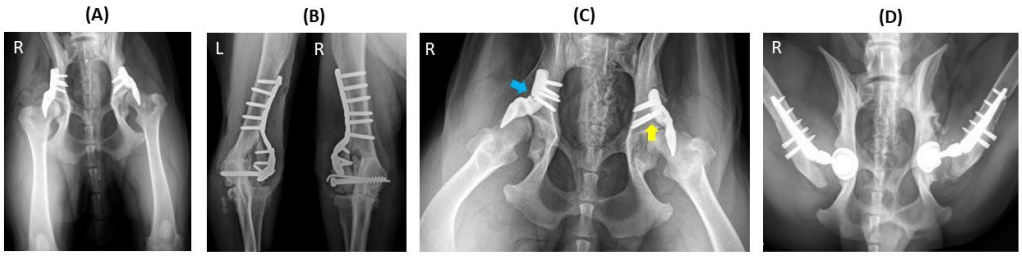

 doi:10.20944/preprints202407.0468.v1

Figure 4. Implant failure of hip no. 23 (left hip) and hip no. 34 (right hip) in a dog that underwent staged bilateral dorsal acetabular rim extension (ACE-X) with a two-month interval. **(A)** The immediate postoperative radiograph showed no complication of the implants' placement with moderate hip osteoarthritis (OA). Five months after the second ACE-X, the dog experienced bilateral humeral condyle fractures requiring humeral plating and screw fixation **(B)**, which was followed by a broken ACE-X implant (blue arrow) and broken screws (yellow arrow) **(C)** and severe OA progression, requiring revision to staged bilateral total hip replacement **(D)**.

Table 4. Comprehensive details of the four dogs (six hips) exhibiting major complications resulting in lameness after dorsal acetabular rim extension.

Parameters		Dog 1		Dog 2	Dog 3		Dog 4
Breed		Newfoundland		Border Collie	German Shepherd dog		Bernese mountain dog
Age at surgery (m)		9	12	7	8		12
Body weight (kg)		38.6	43.7	13.8	26.8		35.6
Hip no.		23	34	37	24	25	53
Side		left	right	right	right	left	right
Lead time (days)		122	107	48	49		74
FCI score		D	E	E	D	E	B
Preoperative NA (°)		87	83	82	94	86	104
Osteophyte size (mm)*	**Visit 1**	2.4	3.4	1.7	1.8	1.9	0
	Visit 2	4.2	4.4	2.3	4	3	0
	Last CT (days)**	6.3 (68)	na	na	7.3 (336)	5.3(91)	3.6 (528)
OA scoring*	**Visit 1**	2	2	1	1	1	0
	Visit 2	2	2	2	2	2	0
	Last CT	3	na	na	3	3	2
Complication		2 broken screws and severe OA	broken implant and severe OA	4 broken screws	severe OA	severe OA	septic arthritis
Follow up time until complication (days)		246	178	215	291	291	528

m: months, kg: kilograms, FCI: the Fédération Cynologique Internationale, NA: Norberg angle, mm: millimeters, OA: osteoarthritis, na: not available, *Osteophyte size and OA score were assessed using CT., **The osteophyte size measured from the last CT (The time interval between the surgery day and the final CT scan was completed.).

Another dog was initially planned for bilateral ACE-X surgery in a single session but experienced a dislocated hip on the day of surgery (visit 2). Consequently, unilateral ACE-X implantation (hip no. 37) was performed, and the contralateral limb underwent THR one month later. Approximately seven months post-ACE-X implantation, the dog developed lameness in the ACE-X treated limb due to four fractured screws necessitating revision surgery involving implant removal and THR (Table 4: Dog 2).

A third dog underwent single-stage bilateral hip surgery (Figure 5B) but experienced significant deterioration in the left hip (hip no.25) approximately 10 months post-ACE-X surgery (Figure 5C), resulting in severe osteoarthritis and pronounced lameness. Subsequent implant removal and THR were performed. Two months later, similar signs emerged in the contralateral hip (hip no. 24) leading to revision surgery at 22 months post-initial ACE-X implantation (Figure 5D and Table 4: Dog 3).

 doi:10.20944/preprints202407.0468.v1

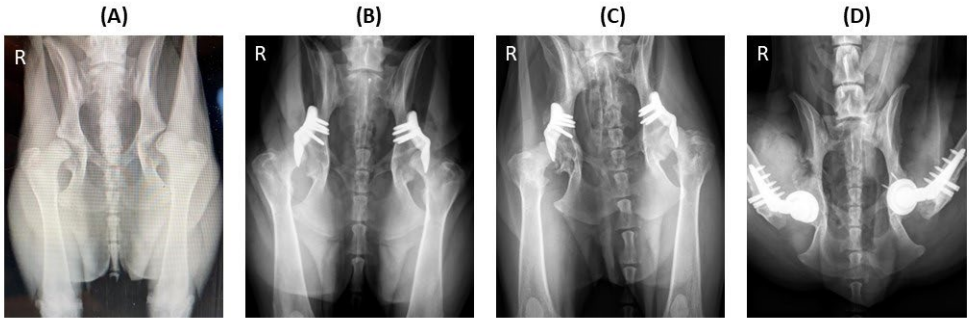

Figure 5. Severe progression of osteoarthritis (OA) after bilateral dorsal ACEtabular rim eXtension (ACE-X; hips no. 24 and 25). Preoperative radiograph **(A)** shows hip dysplasia with hip laxity without OA. Following a 49-day ACE-X lead time, the immediate postoperative radiograph **(B)** shows an increase in laxity and osteophyte formation at both femoral necks. The 10-month follow-up radiograph **(C)** indicates severe progression of OA which required staged bilateral total hip replacement **(D)**.

The last dog initially responded well to bilateral ACE-X implantation for seven months but subsequently developed intermittent lameness in the right hind leg, attributed to a chronic urinary tract infection. Over the course of 7 to 17 months post-ACE-X surgery, the dog underwent surgical cystotomy twice for calculi removal and experienced recurring chronic cystitis episodes coinciding with lameness. Administration of antibiotics significantly improved lameness signs; however, at 17 months post-surgery, consistent lameness persisted in the right hind leg. CT scan revealed characteristic signs of infectious arthritis in the right femoral head and acetabulum (hip no. 53), prompting arthrocentesis and bacterial culture tests. *Staphylococcus pseudointermedius* was isolated from joint fluid and urine samples, leading to the recommendation for staged revision surgery, involving implant removal and joint lavage followed by THR (Table 4: Dog 4).

3.6. Histopathology and 3D X-ray Microscopy

Histopathological examination and 3D X-ray microscopy were utilized to analyze the femoral heads, synovial tissues, and ACE-X implants obtained from the revision hip surgeries. The examination revealed consistent findings across the specimens. The femoral heads showed extensive cartilage loss, particularly in the region where the acetabular rim extension of the implant was located. Additionally, necrosis of denuded subchondral bone with empty lacunae, as well as degeneration of adjacent hyaline cartilage (characterized by fibrillation and fissures), were evident (Figure 6). Histopathological analysis of the synovial tissues demonstrated various alterations, including edema, hyperplasia of synovial lining cells, variable degrees of stromal activation, and the formation of new blood vessels (Figure 7).

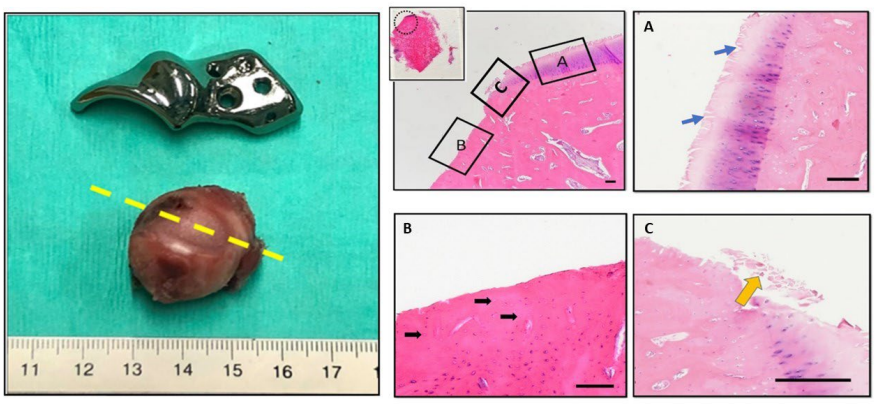

FigureGross examination and histopathological findings of the right femoral head (hip no. 37). The excised femoral head shows significant cartilage loss corresponding to the rim extension part of the

 doi:10.20944/preprints202407.0468.v1

ACE-X implant. Histology sections made at the level of cartilage loss (yellow dash line) and stained with H&E display erosions and denudation of the femoral head. Magnified fields (dotted line circle and rectangular boxes) reveal specific features: Box **A** highlights areas of articular cartilage, blue arrows depict the extension of matrix fibrillation downward and the presence of vertical fissures, Box **B** indicates denudation, complete erosion of the unmineralized hyaline cartilage, black arrows point to empty lacunae suggesting the loss of osteocytes within the subchondral bone tissue, and Box **C** indicates debris of necrotic cartilage tissue (yellow arrow).

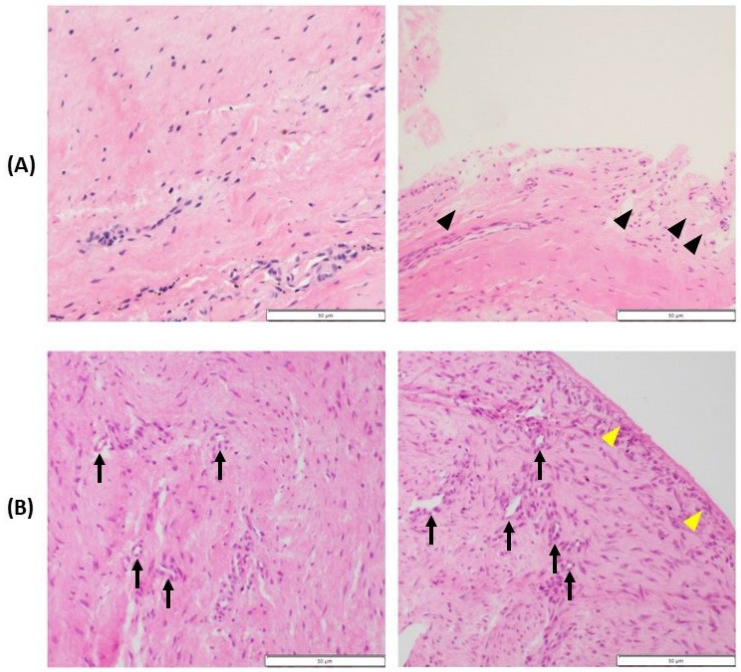

FigureHistopathology of the synovium of hip no. 34 **(A)** and hip no. 37 **(B)**. **(A)** Representative images showing slight activation of the synovial stroma and significant subintimal edema (black arrowheads). **(B)** Micrographs reveal hyperplasia of the synovial intima (yellow arrowheads), marked activation of the synovial stroma (densely located fibroblast and histocytes), and increased vascularization (black arrows).

Upon gross examination, bone integration was observed in the porous surface of the bone attachment part of the removed ACE-X implants at 9 months (hip no. 34) and 22 months (hip no. 24) post-surgery, whereas this integration was not observed in the specimen explanted at 7 months (hip no.37). Three-dimensional X-ray microscopy unveiled bone density within the porous layer of the implant extracted from hip no. 34 at 9 months and hip no. 24 at 22 months post-surgery, while no such density was detected in the control implant (Figure 8B). The original gray values were converted into 3D visualizations with color representation using the TXM3DViewer software (Carl Zeiss X-ray Microscopy Inc., Germany). Each color represented a different attenuation level of the specimen, with red indicating the highest attenuation, followed by orange, yellow, green, and blue in descending order of linear attenuation coefficient. In the control implant, red denoted the highest-density area of the implant, while yellow and green represented lower-density areas. In the removed implants, similar to previous studies, light and dark blue were observed in the porous surface, indicating the density of bone tissue (Figure 8C)[22]. Additionally, histological sections of the removed implant from hip no. 24 showed the presence of newly formed bone characterized by a spongy architecture, consisting of trabeculae with interstitial bone marrow spaces (Figure 9).

 doi:10.20944/preprints202407.0468.v1

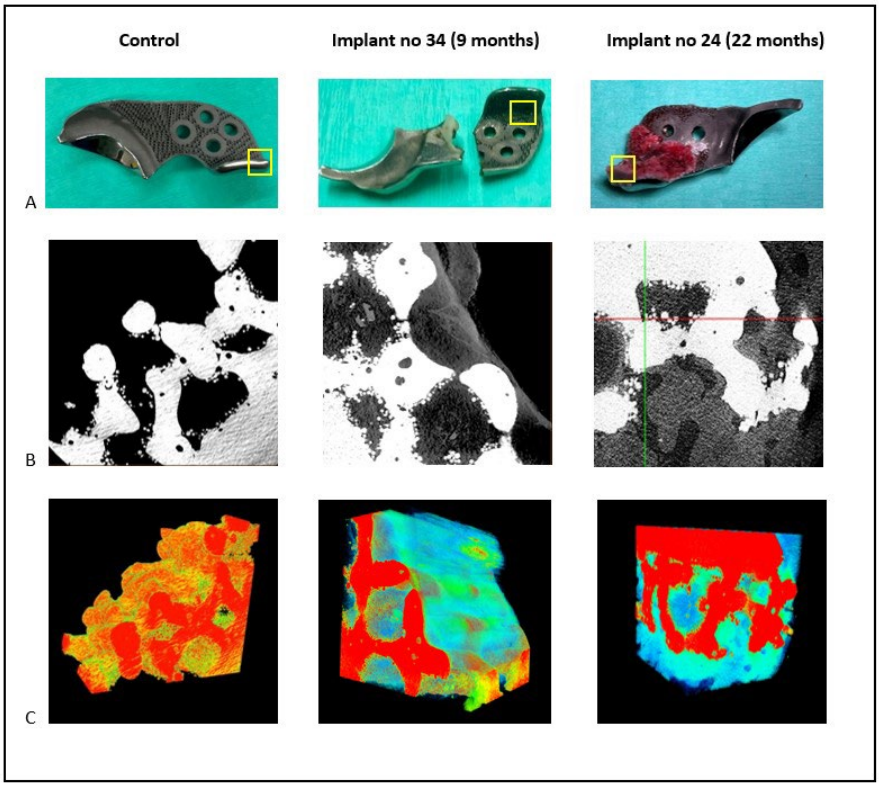

Figure 8. 3D x-ray microscopy of both the control and extracted ACE-X implants (hips no. 34 and 24). **(A)** Images of the implants highlight the study area within the yellow box. **(B)** 2D original imaging displaying varying density areas in gray values. White indicated the high-density zone, while, black indicated the low-density zone. **(C)** 3D reconstruction of the studied area with color visualization representing different density areas. Red indicated the highest density zone, followed by orange, yellow, green, and blue. Trabeculae were depicted in light or dark blue depending on the bone tissue density.

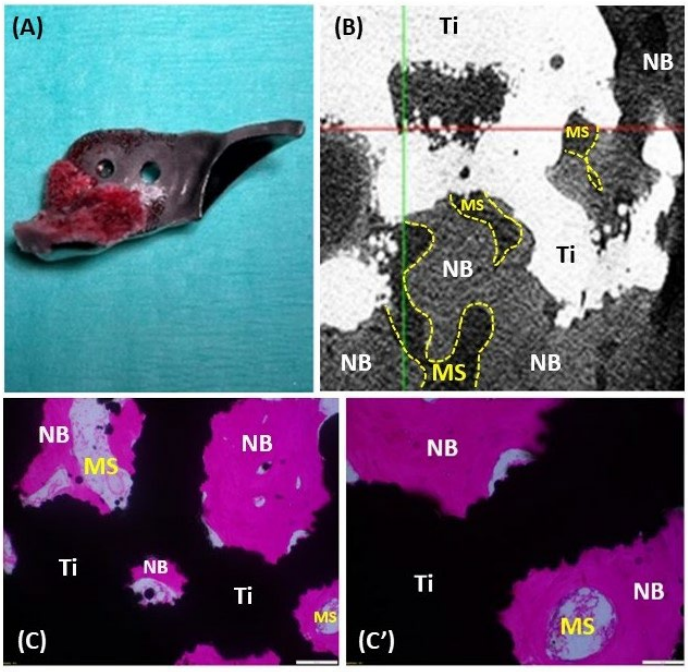

FigureHistology of the removed ACE-X implant (hip no. 24) showing osseointegration at the porous surface. **(A)** The removed ACE-X implant from hip no. 24 at 22 months after surgery. **(B)** 2D X-ray

 doi:10.20944/preprints202407.0468.v1

microscopy image demonstrating new bone formation inside the porous structure of the implant. **(C, C')** Histological images highlighting newly formed bone (NB), bone marrow space (MS), and titanium implant (Ti).

4. Discussion

Hip dysplasia significantly reduces the quality of life for affected dogs due to the inherent laxity of the dysplastic hip, leading to lameness, exercise intolerance, and limb impairment. This study presents the 1-year outcomes of a recently introduced surgical treatment for hip dysplasia using patient-specific 3D-printed titanium implants to extend the dorsal acetabular rim [13]. The ACE-X implant demonstrated effective retention of functionality by expanding femoral head coverage, correcting hip laxity, and reducing pain-related exercise limitations based on owner questionnaires during long-term monitoring.

At the 12-month follow-up, joint laxity evidenced by a positive Ortolani subluxation test was only observed in one hip (hip no. 53), which had consistently shown negative result post-surgery but developed an infectious arthritis secondary to a chronic bladder infection. The change to a positive Ortolani's test is most likely linked to septic arthritis, leading to increased joint fluid and hip joint laxity [23]. Conversely, another hip (hip no. 56) that initially exhibited a positive Ortolani's test at 1.5 months post-surgery displayed a negative result at the 12-month follow-up. This transformation could be attributed to joint capsule thickening [23]. However, with only two exceptions (hips no. 53 and 36), all other dysplastic hips (96.7%) were stable immediately after ACE-X implantation, an observation that is uncommon in DPO-treated hip dysplasia [4], and even more so remained stable at the 12-month evaluation.

Typically, studies on unilateral THR [24,25] and a small cohort of TPO [26] in hip dysplastic dogs demonstrated significant improvement in GRFs of operated limbs at 6 months post-operation, a time point not monitored in this study. The gait pattern study with the aid of force plate analysis returned to baseline levels at a 12-month follow-up in this study, as was reported previously in the study of three experimental dogs with hip dysplasia [12] at 6 months post-surgery. Interestingly, GRFs remained similar to the low baseline values of PVF (40.8 ± 5.9 %BW) and P/T index (0.6 ± 0.1) that were close to the values in healthy dogs (PVF 40.4%, P/T index 0.63) [27]. This could be attributed to the use of low-speed walking (0.8 – 1.3 m/s) during gait analysis, which may not reveal lameness at the preoperative evaluation (visit 1) given that most dogs with HD display lameness after exercise [5,28]. In line with this, others also reported the absence of significant differences in PVF and VI between growing dogs with and without HD [29]. In light of the proposed cut-off value of 19.5% asymmetry indexes as a measure of clinically relevant unilateral lameness [30], the present patient cohort presenting with a 9.6% asymmetry index at the preoperative evaluation, underscores the challenges in detecting substantial changes in gait improvement at early stages of the disease. Despite the absence of detectable improvement at the GRFs level and the confounding bias of the owners' responses due to the open-label design of the study, a decrease in hip joint pain and an improvement in the dogs' exercise capacity was demonstrated from 1.5 months after treatment based on the HCPI owner questionnaire. This outcome is in agreement with findings in dogs that underwent THR, where 64 - 82% of owners reported pain relief according to the owner questionnaires [31–33]. In contrast, owners reported that the dogs undergoing DPO showed weakness during walking in the early postoperative phase [4].

Based on the radiographic measurements, ACE-X implantation significantly increased the femoral head coverage immediately after surgery, with insignificant changes thereafter. These changes are typically related to variations in positioning and are in line with observations in DPO by Vezzoni et al. [4], who reported NA and PC showing non-statistically significant decreases one month post-surgery. Importantly, the measured outcomes consistently fell within the normal range of NA (> 105°), LFO (> 50%), and PC (> 50%) as reported in previous studies [34–36]. When femoral head coverage was assessed, a year following surgery in relation to different HD treatments, ACE-X surgery showed a greater NA at 132 ± 18° than TPO (116 ± 11°) and DPO (106 ± 4°). Furthermore, the PC after ACE-X surgery (77 ± 20%) was higher than that of DPO (65 ± 6%) but similar to TPO (78 ±

 doi:10.20944/preprints202407.0468.v1

20%)[37,38]. These findings suggest that ACE-X surgery provides a coverage level at least comparable to or superior to that achieved through TPO and DPO procedures.

In this study, the osteophyte size significantly progressed at the 12-month follow-up compared to the baseline value, increasing by 0.5 – 1.6 mm, depending on the baseline OA score and the severity of hip laxity. However, a previous study found that osteophyte size increases by 1 mm every three years, as measured by ventrodorsal hip extension radiography [39]. The seemingly faster increase in osteophyte size of the current study could be attributed to differences in measurement methods and tools. Here, osteophyte size was measured using 1 mm sections of both coronal and transverse CT of the hip joint, which provided superior details for accurate measurements and improved early detection of OA [40,41]. When the dogs were categorized based on the baseline OA score on CT and FCI score on radiographs, those with an OA score of 2 showed the highest progression of osteophyte size (1.6 ± 1.3 mm). Furthermore, the dogs with an FCI score of E exhibited the highest progression of osteophyte size (1.6 ± 1.4 mm). Altogether these findings suggest that dogs with moderate to severe OA development and/or high laxity score of the hip joint may not be suitable candidates for ACE-X treatment.

Examination of three implants through X-ray microscopy revealed osseointegration into the porous surface at least by 9 months post-implantation. According to a study on THR, osseointegration of the noncoated 3D-printed porous titanium alloy acetabular cup was observed within a month after implantation [42]. Slower implant-bone integration rates of the noncoated ACE-X implant may be attributed to the direct placement of the implant over the cortical bone of the iliac body. Despite utilizing a periosteal elevator to prompt periosteal reaction, the mesenchymal stem cells released through this method are probably not as plentiful as those originating from the bone marrow, as observed in the THR procedure exposing the acetabular cancellous bone. Several avenues can improve osteointegration, including (a) Osteostimulation (e.g., osteostixis) at the implant placement site to initiate bleeding facilitating the migration of mesenchymal stem cells to the bone-implant interface [43], (b) the use of surface coatings such as hydroxyapatite or other bioactive materials mimicking the composition of natural bone and promoting osteoblast activity, and (c) coatings modulating the inflammatory response and stimulate bone formation at the implant-bone interface [44–46]. Noteworthy, the available data on osseointegration in the ACE-X implant came from dogs that had complications, which could have slowed down the integration of the bone into the implant and produced biased results. Additionally, stability was seen in other ACE-X implants on radiographs and CT scans, indicating that osseointegration may have occurred in clinically sound dogs earlier than the 9-month post-surgery mark.

Complications following ACE-X implantation were reported in this study, with an overall postoperative complication rate of 14.8% and major complication rate of 9.8% requiring revision. This rate was notably lower than those reported for other procedures as TPO, which had a complication rate of 33% [5] and DPO, with a rate of 20.7% [4]. The lower incidence of complications in ACE-X can be attributed to the less invasive surgical approach, eliminating the need for osteotomy to reshape the acetabulum, preserving the natural pelvic canal, and mitigating the risk of delayed or non-union of the bone. Risk factors associated with severe complications following ACE-X implantation included pronounced hip laxity, accelerated OA progression, and marked forelimb lameness. Moreover, in the event of ACE-X failure, a salvage THR presents a viable alternative that yields positive outcomes, as opposed to DPO/TPO, where implant failure may lead to severe complications, irreversible impairment of limb functions, and the added challenge of revision surgery [8]. Of note, three implant failures were observed in this study. Two failures occurred in a dog with bilateral humeral condyle fractures five months post-ACE-X implantation. The third failure was in a dog with contralateral hip luxation, who underwent THR six weeks after ACE-X implantation. In these patients, implant failure may result from the overstress placed on the implant as a result of implant overload. Therefore, ensuring critical case selection at the time of inclusion and preventing concurrent injuries during the initial osseointegration phase is essential for the long-term success of the implant.

This study has several limitations to consider. Being the initial clinical investigation employing the ACE-X implant in client-owned dogs, a wide spectrum of dogs affected by HD were enrolled,

 doi:10.20944/preprints202407.0468.v1

which might have contributed to a higher complication rate due to inappropriate case selection (i.e.; moderate OA development and severe hip laxity). The advancement of OA to a severe stage in certain dogs was also influenced by a delay in implant manufacturing, possibly exacerbated by COVID-related disruptions. Furthermore, 26% of dog patients did not complete the 12-month follow-up, which could have introduced bias into the results. Hence, future studies should implement strict inclusion criteria, concentrating on dogs with mild to moderate hip laxity, and minimal or no preoperative OA development, as determined by preoperative CT scans. Moreover, efforts should be made to reduce the manufacturing (lead) time of the implant to 2 – 4 weeks. Moreover, given the intended lifelong placement of ACE-X implants in dogs, extended follow-up utilizing owner questionnaires and imaging surveillance is imperative for accurately assessing long-term outcomes.

5. Conclusions

In conclusion, the utilization of the ACE-X implant in dogs with hip dysplasia offers a comprehensive array of benefits. These include increased coverage of the femoral head, improved support and stability for the dysplastic hip joint, alleviated hip pain and dysfunction, reduced surgical and recovery durations, and reduced postoperative complications due to the less invasive surgical approach. The enhanced joint stability provided by the ACE-X implant diminishes the risk of subluxation or dislocation, ultimately leading to decrease discomfort and dysfunction in HD-affected dogs. The customization and precision of ACE-X implants, tailored to individual canine anatomy, provide optimal fit, thereby minimizing complications and maximizing effectiveness. Furthermore, the reduced invasiveness of ACE-X implantation, preserving the joint and minimizing soft tissue trauma, allows for bilateral simultaneous procedures and necessitates a shorter postoperative recovery period compared to traditional methods. Notably, the lower reported complication rate associated with ACE-X implantation, which may be further minimized by strict inclusion criteria and reduction of implant lead time, renders it a valuable and promising treatment option for enhancing joint stability, correcting dysplastic anatomy, and improving overall quality of life in young dogs with hip dysplasia. Consequently, the ACE-X implant emerges as a secure and valuable option for clinical application

Author Contributions: BM: BvdW, RS, and MT were involved conception and design of the study. Surgeries were performed by BM and IK. Data collection was carried out by IK and BM. Implants were designed by KW and JM. IK organized the database, conducted statistical analysis, and drafted the initial manuscript. AK handled tissue samples and reported histopathological results, and YJ conducted 3D x-ray microscope analysis. Sections of the manuscript were written by AK, YI, and FV. All authors contributed to manuscript revisions, reviewed, and approved the final version for submission. All authors have read and agreed to the published version of the manuscript.

Funding: The research received financial support from various grants, including the European Investment funds Interreg VA Flanders, endorsed by the Ministry of Economic Affairs (NL) and the Provinces Limburg (NL) and Flemish-Brabant (B) for the PRosPERoS (PRinting PERsonalized orthopaedic implantS) project. Additionally, funding was provided by charity funds allocated to Friends of VetMed (Vrienden Diergeneeskunde) for the execution of the clinical dog study, including contributions from the K.F.Hein Fonds; Dinamo Fonds; Stichting Nijdier; Stichting Meijer Boekbinder Fonds, and Stichting Het Waardige Dier. Moreover, this research received financial support from the Dutch Arthritis Society (LLP22 and LLP12). The CT instrument at the Multi-scale Imaging and Tomography Facility (MINT) at Utrecht University was funded by the Netherlands Research Council (NWO) via the EPOS-NL Research Infrastructure program. Furthermore, IK is a recipient of a scholarship from the Faculty of Veterinary Medicine, Kasetsart University, Thailand.

Institutional Review Board Statement: The study protocol was approved by the Veterinary Clinical Studies Committee, Utrecht University, Utrecht, The Netherlands. This study is considered a non-experimental clinical veterinary practice as mentioned in Article 1 – 5(b) of Directive 2010/63/EU. Throughout the study, the dogs remained under the supervision and care of their owners.

Informed Consent Statement: Informed consent was obtained from all owners involved in the study.

Data Availability Statement: The data presented in this study are available within the article. Raw data supporting this study are available from the corresponding author by request.

Acknowledgments: We extend our gratitude to Saskia G.M. Plomp for her technical assistance and expertise in histopathology preparation, as well as to Inger Laponder for her diligent patient management. Our sincere appreciation also goes to the owners of dogs with hip dysplasia, veterinary students, referring veterinarians, and veterinary technicians whose contributions were invaluable to this study.

Conflicts of Interest: The authors have no conflicts of interest to declare. BM, BvdW, and RS are inventors of the method of manufacturing an implant to extend the dorsal acetabular rim (2021) of which the patent (EP3463198B1) has been licensed to Rita Leibinger.

References

1. Loder RT, Todhunter RJ. The Demographics of Canine Hip Dysplasia in the United States and Canada. J Vet Med. (2017):5723476. doi: 10.1155/2017/5723476
2. Demko J, McLaughlin R. Developmental Orthopedic Disease. Veterinary Clinics of North America: Small Animal Practice. (2005) 35(5):1111-35. doi: 10.1016/j.cvsm.2005.05.002
3. Dueland RT, Adams WM, Patricelli AJ, Linn KA, Crump PM. Canine hip dysplasia treated by juvenile pubic symphysiodesis. Part I: two year results of computed tomography and distraction index. Vet Comp Orthop Traumatol. (2010) 23(5):306-17. doi: 10.3415/VCOT-09-04-00454.
4. Vezzoni A, Boiocchi S, Vezzoni L, Vanelli AB, Bronzo V. Double pelvic osteotomy for the treatment of hip dysplasia in young dogs. Vet Comp Orthop Traumatol. (2010) 23(6):444-52. doi: 10.3415/VCOT-10-03-0034
5. Koch DA, Hazewinkel HAW, Nap RC, Meij BP, Wolvekamp WTC. Radiographic Evaluation and Comparison of Plate Fixation after Triple Pelvic Osteotomy in 32 Dogs with Hip Dysplasia. Vet Comp Orthop Traumatol. (1993) 06(01):09-15. doi: 10.1055/s-0038-1633049
6. Johnson AL, Smith CW, Pijanowski GJ, Hungerford LL. Triple pelvic osteotomy: effect on limb function and progression of degenerative joint disease. J Am Anim Hosp Assoc. (1998) 34(3):260-4. doi: 10.5326/15473317-34-3-260
7. Slocum B, Slocum TD. Current techniques in small animal surgery: Baltimore: Williums & Wilkings (1998).
8. Vezzoni A. Complications of Double and Triple Pelvic Osteotomies. Complications in Small Animal Surgery. (2016) 759-77. doi: 10.1002/9781119421344
9. Tong K, Hayashi K. Obturator nerve impingement as a severe late complication of bilateral triple pelvic osteotomy. Vet Comp Orthop Traumatol. (2012) 25(1):67-70. doi: 10.3415/VCOT-11-03-0039
10. Jensen DJ, Sertl GO. Sertl shelf arthroplasty (BOP procedure) in the treatment of canine hip dysplasia. Vet Clin North Am Small Anim Pract. (1992) 22(3):683-701. doi: 10.1016/s0195-5616(92)50062-6
11. Lussier B, Lanthier T, Martineau-Doizé B. Evaluation of biocompatible osteoconductive polymer shelf arthroplasty for the surgical correction of hip dysplasia in normal dogs. Can J Vet Res. (1994) 58(3):173-80.
12. Willemsen K, Tryfonidou MA, Sakkers RJB, Castelein RM, Beukers M, Seevinck PR, et al. Patient-specific 3D-printed shelf implant for the treatment of hip dysplasia tested in an experimental animal pilot in canines. Sci Rep. (2022) 12(1):3032. doi: 10.1038/s41598-022-06989-9
13. Kwananocha I, Magré J, Willemsen K, Weinans H, Sakkers RJB, How T, et al. Acetabular rim extension using a personalized titanium implant for treatment of hip dysplasia in dogs: short-term results. Frontiers in Veterinary Science. (2023) 10:1160177. doi: 10.3389/fvets.2023.1160177
14. Fédération Cynologique Internationale, Brass W, Paatsama S. Hip Dysplasia: International Certificate and Evaluation of Radiographs: Helsinki: F.C.I. (1983).
15. Meomartino L, Fatone G, Potena A, Brunetti A. Morphometric assessment of the canine hip joint using the dorsal acetabular rim view and the centre-edge angle. J Small Anim Pract. (2002) 43(1):2-6. doi: 10.1111/j.1748-5827.2002.tb00001.x
16. Fluckiger M. Scoring Radiographs for Canine Hip Dysplasia-The Big Three Organisations in the World. European Journal of Compagnion Animal Practice. (2007) 2:135-40.
17. Butler JR, Gambino J. Canine Hip Dysplasia: Diagnostic Imaging. Vet Clin North Am Small Anim Pract. (2017) 47(4):777-93. doi: 10.1016/j.cvsm.2017.02.002
18. Lavrijsen IC, Heuven HC, Voorhout G, Meij BP, Theyse LF, Leegwater PA, et al. Phenotypic and genetic evaluation of elbow dysplasia in Dutch Labrador Retrievers, Golden Retrievers, and Bernese Mountain dogs. Vet J. (2012) 193(2):486-92. doi: 10.1016/j.tvjl.2012.01.001
19. Willemsen K, Tryfonidou M, Sakkers R, Castelein RM, Zadpoor AA, Seevinck P, et al. Patient-specific 3D-printed shelf implant for the treatment of hip dysplasia: Anatomical and biomechanical outcomes in a canine model. J Orthop Res. (2021) 40(5):1154-1162. doi: 10.1002/jor.25133
20. Hielm-Björkman AK, Kuusela E, Liman A, Markkola A, Saarto E, Huttunen P, et al. Evaluation of methods for assessment of pain associated with chronic osteoarthritis in dogs. J Am Vet Med Assoc. (2003) 222(11):1552-8. doi: 10.2460/javma.2003.222.1552

21. Hielm-Björkman AK, Rita H, Tulamo RM. Psychometric testing of the Helsinki chronic pain index by completion of a questionnaire in Finnish by owners of dogs with chronic signs of pain caused by osteoarthritis. Am J Vet Res. (2009) 70(6):727-34. doi: 10.2460/ajvr.70.6.727
22. Van Oossterwyck H, Duyck J, Vander Sloten J, Van der Perre G, Jansen J, Wevers M, et al. Use of microfocus computerized tomography as a new technique for characterizing bone tissue around oral implants. J Oral Implantol. (2000) 26(1):5-12. doi: 10.1563/1548-1336(2000)026<0005:TUOMCT>2.3.CO;2
23. Vidoni B, Bauer V, Bockstahler B, Gumpenberger M, Tichy A, Aghapour M. Early Diagnosis of Canine Hip Laxity: Correlation between Clinical Orthopedic Examinations and the FCI Scoring Method in a Closed Cohort of Rottweilers. Animals (Basel). (2021) 11(2). doi: 10.3390/ani11020416
24. Budsberg SC, Chambers JN, Lue SL, Foutz TL, Reece L. Prospective evaluation of ground reaction forces in dogs undergoing unilateral total hip replacement. Am J Vet Res.
25. (1996) 57(12):1781-5.
26. Braden TD, Olivier NB, Blaiset MA, Averill, Samantha, Bolliger CT, Decamp CE. Objective evaluation of total hip replacement in 127 dogs utilizing force plate analysis. Veterinary and Comparative Orthopaedics and Traumatology. (2004) 17:78-81. doi: 10.1055/s-0038-1636477
27. McLaughlin RM, Jr., Miller CW, Taves CL, Hearn TC, Palmer NC, Anderson GI. Force plate analysis of triple pelvic osteotomy for the treatment of canine hip dysplasia. Vet Surg. (1991) 20(5):291-7. Doi: 10.1111/j.1532-950x.1991.tb01270.x
28. Suwankong N, Meij BP, Van Klaveren NJ, Van Wees AM, Meijer E, Van den Brom WE, et al. Assessment of decompressive surgery in dogs with degenerative lumbosacral stenosis using force plate analysis and questionnaires. Vet Surg. (2007) 36(5):423-31. doi: 10.1111/j.1532-950X.2007.00288.x
29. Fry TR, Clark DM. Canine hip dysplasia: clinical signs and physical diagnosis. Vet Clin North Am Small Anim Pract. (1992) 22(3):551-8. doi: 10.1016/s0195-5616(92)50055-9.
30. Virag Y, Gumpenberger M, Tichy A, Lutonsky C, Peham C, Bockstahler B. Center of pressure and ground reaction forces in Labrador and Golden Retrievers with and without hip dysplasia at 4, 8, and 12 months of age. Front Vet Sci. (2022) 9:1087693. doi: 10.3389/fvets.2022.1087693
31. Fanchon L, Grandjean D. Accuracy of asymmetry indices of ground reaction forces for diagnosis of hind limb lameness in dogs. Am J Vet Res. (2007) 68(10):1089-94. doi: 10.2460/ajvr.68.10.1089
32. Skurla CT, Egger EL, Schwarz PD, James SP. Owner assessment of the outcome of total hip arthroplasty in dogs. J Am Vet Med Assoc. (2000) 217(7):1010-2. doi: 10.2460/javma.2000.217.1010
33. Allaith S, Tucker LJ, Innes JF, Arthurs G, Vezzoni A, Morrison S, et al. Outcomes and complications reported from a multiuser canine hip replacement registry over a 10-year period. Vet Surg. (2023) 52(2):196-208. doi: 10.1111/vsu.13885
34. Forster KE, Wills A, Torrington AM, Moores AP, Thomson D, Arthurs G, et al. Complications and owner assessment of canine total hip replacement: a multicenter internet based survey. Vet Surg. (2012) 41(5):545-50. doi: 10.1111/j.1532-950X.2012.01015.x
35. Gaspar AR, Hayes G, Ginja C, Ginja MM, Todhunter RJ. The Norberg angle is not an accurate predictor of canine hip conformation based on the distraction index and the dorsolateral subluxation score. Prev Vet Med. (2016) 135:47-52. doi: 10.1016/j.prevetmed.2016.10.020
36. Janssens L, De Ridder M, Verhoeven G, Gielen I, van Bree H. Comparing Norberg angle, linear femoral overlap and surface femoral overlap in radiographic assessment of the canine hip joint. J Small Anim Pract. (2014) 55(3):135-8. doi: 10.1111/jsap.12171
37. Tomlinson JL, Johnson JC. Quantification of measurement of femoral head coverage and Norberg angle within and among four breeds of dogs. Am J Vet Res. (2000) 61(12):1492-500. doi: 10.2460/ajvr.2000.61.1492
38. Borostyankoi F, Rooks RL, Kobluk CN, Reed AL, Littledike ET. Results of single-session bilateral triple pelvic osteotomy with an eight-hole iliac bone plate in dogs: 95 cases (1996-1999). J Am Vet Med Assoc. (2003) 222(1):54-9. doi: 10.2460/javma.2003.222.54
39. Petazzoni M, Tamburro R. Clinical outcomes of double pelvic osteotomies in eight dogs with hip dysplasia aged 10-28 months. Vet Surg. (2022) 51(2):320-9. doi: 10.1111/vsu.13737
40. Greene LM, Marcellin-Little DJ, Lascelles BD. Associations among exercise duration, lameness severity, and hip joint range of motion in Labrador Retrievers with hip dysplasia. J Am Vet Med Assoc. (2013) 242(11):1528-33. doi: 10.2460/javma.242.11.1528
41. Kunst CM, Pease AP, Nelson NC, Habing G, Ballegeer EA. Computed tomographic identification of dysplasia and progression of osteoarthritis in dog elbows previously assigned OFA grades 0 andVet Radiol Ultrasound. (2014) 55(5):511-20. doi: 10.1111/vru.12171
42. Andronescu AA, Kelly L, Kearney MT, Lopez MJ. Associations between early radiographic and computed tomographic measures and canine hip joint osteoarthritis at maturity. Am J Vet Res. (2015) 76(1):19-27. doi: 10.2460/ajvr.76.1.19
43. Bai X, Li J, Zhao Z, Wang Q, Lv N, Wang Y, et al. In vivo evaluation of osseointegration ability of sintered bionic trabecular porous titanium alloy as artificial hip prosthesis. Front Bioeng Biotechnol. (2022) 10:928216. doi: 10.3389/fbioe.2022.928216

 doi:10.20944/preprints202407.0468.v1

44. Mirza MZ, Swenson RD, Lynch SA. Knee cartilage defect: marrow stimulating techniques. Curr Rev Musculoskelet Med. (2015) 8(4):451-6. doi: 10.1007/s12178-015-9303-x
45. Chamrad J, Marcián P, Cizek J. Beneficial osseointegration effect of hydroxyapatite coating on cranial implant - FEM investigation. PLoS One. (2021) 16(7):e0254837. doi: 10.1371/journal.pone.0254837
46. Schünemann FH, Galárraga-Vinueza ME, Magini R, Fredel M, Silva F, Souza JCM, et al. Zirconia surface modifications for implant dentistry. Mater Sci Eng C Mater Biol Appl. (2019) 98:1294-305. doi: 10.1016/j.msec.2019.01.062
47. Wang Y, Wang J, Gao R, Liu X, Feng Z, Zhang C, et al. Biomimetic glycopeptide hydrogel coated PCL/nHA scaffold for enhanced cranial bone regeneration via macrophage M2 polarization-induced osteo-immunomodulation. Biomaterials. (2022) 285:121538. doi: 10.1016/j.biomaterials.2022.121538